riods when the lake became shallow and vegetation on the lower slopes became more open. *Sarcobatus* and Cyperaceae spread over the exposed flats, and *Sparganium* expanded in the shallower water. Pine forests along the lower slope were replaced by a more open pine woodland that featured at different times *Artemisia*, Gramineae, and herbs in the understory and possibly *Juniperus* at its lower edge. At the same time the contribution from hardwoods growing in the valleys increased in the pollen record. The three arid periods are estimated to have lasted 5000 to 50,000 years (inferred from T2), 21,000 to 210,000 years (T4), and 2000 to 20,000 years (T6). The intervening wetter intervals lasted 1000 to 11,000 years (T3) and 1000 to 10,000 years (T5).

Pollen data from the Teewinot Formation help pinpoint the increase in continentality in the Rocky Mountains in the late Tertiary. Older Neogene floras in the western United States contain conifer assemblages with notable subtropical and temperate elements (*9, 10*), but the Teewinot record shows that the extirpation of these early Tertiary relicts was nearly complete in the Rocky Mountains by 9 million years ago (*11*). In northwestern Wyoming, post-Teewinot assemblages show an essentially modern flora by late Blancan (latest Pliocene) time (*12*). Epeirogeny, creation of orographic barriers to maritime air masses from the Pacific Ocean, and global climatic cooling all contributed to the development of drier conditions and greater seasonality in the West during the late Tertiary (*13*).

The vegetation reconstructions derived from the pollen data of this one interval of the Teewinot Formation suggest that climatic oscillations, each with a time span lasting between 1000 and 200,000 years, have occurred repeatedly during the late Miocene. These findings suggest that the Tertiary lake deposits such as the Teewinot Formation have the potential to reveal the nature of pre-Quaternary climatic variability.

CATHY W. BARNOSKY*
Department of Geological Sciences, University of Washington, Seattle 98195

References and Notes

1. J. Kennett, in *Paleoecology of Africa* 6, E. van Zinderen-Bakker, Ed. (Balkema, Cape Town, South Africa, 1975), pp. 59–78; L. Keigwin, *Earth Planet. Sci. Lett.* **45**, 361 (1979); F. Woodruff, S. M. Savin, R. G. Douglas, *Science* **212**, 665 (1981).
2. J. D. Love and J. C. Reed, Jr., *Creation of the Teton Landscape* (Grand Teton Natural History Association, Moose, Wyo., 1971); D. W. Taylor, in *Guidebook, 11th Annual Field Conference* (Wyoming Geological Society, Laramie, 1956), p. 123; I. Sohn, in *ibid.*, p. 120.
3. J. Evernden, D. Savage, G. Curtis, G. James, *Am. J. Sci.* **262**, 145 (1974); C. Hibbard, *Contrib. Mus. Paleontol. Univ. Mich.* **23**, 95 (1970); C. Repenning, *Can. J. Anthropol.* **1**, 37 (1980).
4. J. D. Love, in *Guidebook, 29th Annual Field Conference* (Wyoming Geological Society, Laramie, 1977), p. 585.
5. W. H. Bradley [in *Limnology in North America*, D. Frey, Ed. (Univ. of Wisconsin Press, Madison, 1966), pp. 621–652] suggested a rate of 1 m per 6000 years for the accumulation of freshwater laminated marlstone. D. E. Schindel [*Paleobiology* **6**, 408 (1980)], on the other hand, estimated a rate of only 1 m per 170 years from the accumulation of the most recent uncompacted sediment in large deep lakes, such as Lake Superior. These basins are poor analogs for the Teewinot system, however, and the only dated sedimentary records considered here are those from large shallow lakes in temperate latitudes. The sources used are Quaternary lake sediments in Turkey, Greece, Iran, Syria, and the southwestern United States. [W. van Zeist, H. Woldring, D. Stapert, *Palaeohistoria* **17**, 53 (1975); S. Bottema, thesis, University of Groningen (1974); T. van der Hammen, T. Wijmstra, W. Zagwijn, in *Late-Cenozoic Glacial Ages*, K. Turekian, Ed. (Yale Univ. Press, New Haven, Conn., 1971), pp. 391–424; W. van Zeist and S. Bottema, *Palaeohistoria* **19**, 19 (1977); J. Niklewski and W. van Zeist, *Acta Bot. Neerl.* **19**, 737 (1970); M. Stuiver and G. Smith, *U.S. Geol. Surv. Prof. Pap. 1043* (1979), p. 68].
6. Samples were processed by methods described by I. Doher [*U.S. Geol. Surv. Circ. 830* (1980)]. About 300 grains were identified in each sample, and percentages were calculated on the basis of total terrestrial pollen.
7. Basic methodology and application are discussed in H. J. B. Birks and H. H. Birks [*Quaternary Paleoecology* (Arnold Press, London, 1980), pp. 196–206].
8. Cupressaceae pollen was separated from that of Taxaceae and Taxodiaceae by its two-split form and irregularly scattered gemmae and by the absence of an exitus papilla.
9. E. Leopold and H. MacGinite, in *Floristics and Paleofloristics of Asia and Eastern North America*, A. Graham, Ed. (Elsevier, Amsterdam, 1972), pp. 147–200.
10. H. Becker, *Geol. Soc. Am. Mem.* **82**, 127 (1961); D. Axelrod, *Univ. Calif. Publ. Geol. Sci.* **59**, 83 (1964); H. MacGinite, *ibid.* **35**, 67 (1962); R. Taggart and A. Cross, in *Biostratigraphy of Fossil Plants*, D. Dilcher and T. Taylor, Eds. (Hutchinson & Ross, New York, 1980), pp. 185–210.
11. Interpretations agree with those of E. Leopold [in *Pleistocene Extinctions: the Search for a Cause*, P. Martin and H. Wright, Eds. (Yale Univ. Press, New Haven, Conn., 1967), pp. 203–246.]
12. C. W. Barnosky, unpublished data.
13. D. Rasmussen, *Northwest Geol.* **2**, 27 (1973); J. D. Love, *Am. J. Sci.* **258A**, 204 (1960); J. Clark, *Geol. Soc. Am. Mem.* **144**, 95 (1975); G. Thompson, R. Fields, D. Alt, *Geology* **10**, 413 (1982).
14. I thank E. B. Leopold, J. D. Love, H. E. Wright, and A. D. Barnosky for discussions and comments on the manuscript; K. Haffnieter for laboratory assistance; the University of Wyoming–National Park Service Research Center for providing laboratory and field facilities; and the National Elk Refuge. Supported by an NSF graduate fellowship.
* Present address: School of Botany, Trinity College, Dublin 2, Ireland.

14 March 1983; accepted 1 April 1983

Turbulent Jets and Eddies in the California Current and Inferred Cross-Shore Transports

Abstract. *The instantaneous California Current is seen to consist of intense meandering current filaments (jets) intermingled with synoptic-mesoscale eddies. These quasi-geostrophic jets entrain cold, upwelled coastal waters and rapidly advect them far offshore; this behavior accounts for the elongated, cool surface features that are seen extending across the California Current region in satellite infrared imagery. The associated advective mechanism should provide significant cross-shore transports of heat, nutrients, biota, and pollutants. The dynamics of the current system should be crucially influenced by its highly variable structure.*

The California Current is the major eastern boundary current of the North Pacific. Its flow regime is important for fisheries and climate-related processes; for oil and gas recovery operations and waste disposal; for biological, chemical, and geological investigations; and for physical oceanographic studies. Nonetheless, the role of this current in the general circulation is not clear and its kinematics and internal dynamics have not been established. Such eastern boundary currents have generally been thought to be broad, shallow, and slow (*1, 2*), although some reports (*3*) of eddies, generally based on sparse information, do exist.

In a sequence of three quasi-synoptic studies conducted in March through August 1982, we mapped hydrographic fields with high spatial resolution within a domain 160 by 200 km in the California Current System (CCS). The flows that we observed did not consist of the previously conceived steady southward drift; instead, they were highly variable in space and time and were dominated by variously oriented jetlike strong current filaments and eddies. Preliminary results are presented here to provide new, relevant kinematic concepts and to aid in the interpretation of satellite infrared imagery from such regions. These studies initiated acquisition of a database in a "test block" of ocean established to provide the basis for a statistical-dynamical eddy-resolving model system for ocean prediction in general (*4*), and to provide for a dynamical analysis of the role of the eddies in the CCS (CCS is used here to connote an aggregate of flows: the California Current, the California Undercurrent, associated eddies, and transients, which coexist and intermingle along the West Coast). This effort was an early step in the Naval Postgraduate School–Harvard OPTOMA (Ocean Prediction Through Observations, Mod-

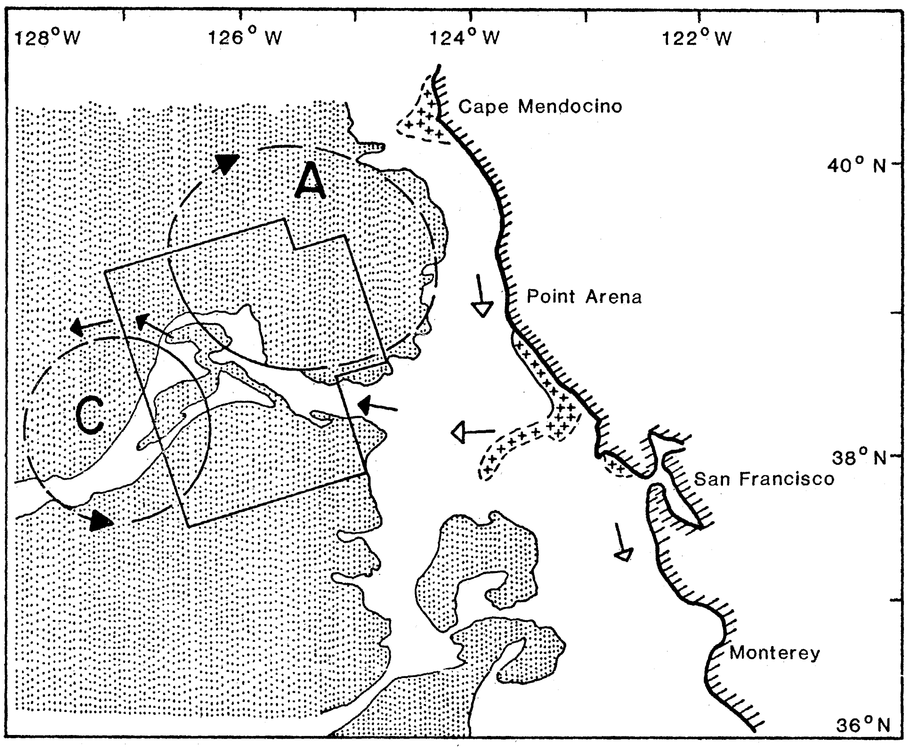

Fig. 1. The union of the study domains for CCS2, leg I (1 to 4 August 1982), and CCS2, leg II (9 to 12 August 1982), is outlined (see Fig. 2). Superimposed are schematized positions of the jet and synoptic-scale eddies for CCS2, leg I, and their logical extrapolations; *C*, cyclonic eddy; *A*, anticyclonic eddy. Arrows indicate principal surface flows; solid arrows are definite and open arrows are inferential. Also shown is a qualitative analysis of satellite infrared image gray shades for sea-surface temperature (SST) predominant patterns on 1 August 1982: coolest SST, crosses; warmest SST, dots.

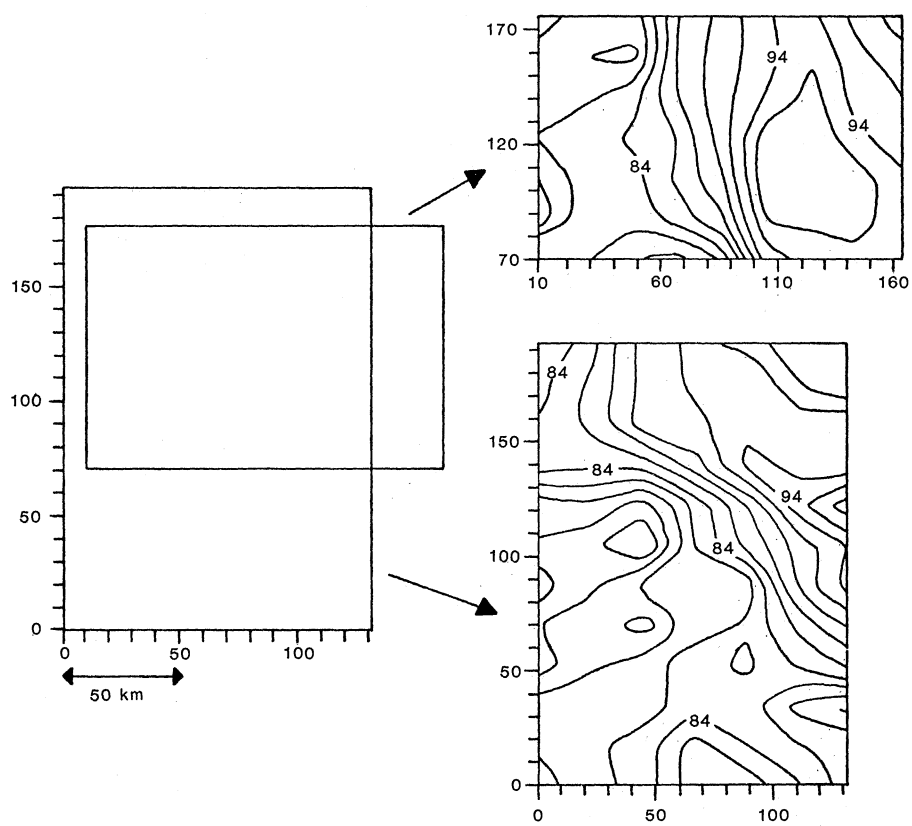

Fig. 2. Surface dynamic topography relative to 450 m. On the left is the superposition of the CCS2, leg I (the larger), and CCS2, leg II, study domains. The surface dynamic topography is contoured at intervals of 2 dynamic centimeters. The surface geostrophic flow is along contours to the right when facing from high to low values.

eling, and Analysis) Program. The three quasi-synoptic (that is, the regime varied somewhat over the duration of sampling) studies are labeled CCS1 (8 to 12 March 1982), CCS2, leg I (1 to 4 August 1982), and CCS2, leg II (9 to 12 August 1982). They acquired, respectively, 99, 85, and 82 expendable bathythermograph (XBT) casts to 450 m and 0, 26, and 37 conductivity-temperature-depth (CTD) casts to between 500 and 1500 m, within a domain centered about 150 km offshore of Northern California (Fig. 1).

The characteristics of the grid of observations for CCS2, leg I, illustrate the sampling strategy. Relatively high-resolution (9 km) sampling was done along four lines spaced 40 km apart and oriented more or less parallel to the coast [in contrast to the usual cross-shore orientation of hydrographic lines (*2*)]. Our strategy allowed for the subsurface resolution of prominent features of the cross-shore sea-surface temperature (SST) indicated in satellite infrared imagery. For calculating density and dynamic height profiles from the XBT's we inferred salinity profiles from the temperature profiles using mean temperature-salinity curves for the region based on California Cooperative Oceanic Fisheries Investigations hydrographic casts, since the mean temperature-salinity curve calculated from the CCS2 CTD data agreed closely with that mean. To describe the surface geostrophic flow, the dynamic height of the surface was computed relative to 450 m, consistent with the traditional regional geostrophic reference level of 500 dbar (500 m). Although recent direct current measurements south of Mendocino Escarpment indicate deep (presumably geostrophic) flows of 5 cm sec^{-1} or greater with time scales of a few months (*5*) and suggest a variable reference level, our picture of the main thermocline-to-surface flow should be reliable.

Quasi-synoptic maps of surface dynamic topography for CSS2, leg I and leg II, illustrate the geostrophic jet and eddy fields (Fig. 2). In CCS2, leg I, the general pattern contained a jet 40 km wide with speeds up to 50 cm sec^{-1} flowing northwest (opposite to the climatological mean California Current). This jet was formed by the joining of two branches, one originating in the southeast and the other in the southwest. It weakened with depth and extended to a few hundred meters, that is, throughout the main thermocline. The volume transport of the jet was about 2 sverdrups (2×10^6 m^3 sec^{-1}), which is about 20 percent of that of the climatological mean California Current. The flows on either side of the jet were consistent with a major pair of counterrotating [one anticyclonic (high) and one cyclonic (low)] eddies; smaller mesoscale eddies were also present within the domain. In CCS2, leg II, the jet had a more alongshore orientation and its intensity had changed. The changes in jet orientation and intensity were consistent with (i) northwestward displacement of the main cyclonic eddy at a rate of 8 to 12 km per day; (ii) westward displacement of the main anticyclonic eddy at rate of 2 to 4 km per day; and (iii) westward dispersion of the jet, at a rate of 3 to 5 km per day, in the "wake" of the cyclonic eddy. In CCS1, the general pattern (not shown) was a branching jet flowing from northwest to southeast with smaller mesoscale eddies 15 to 30 km in diameter and indications of larger (100 to 200 km) features centered outside the domain. In each quasi-synoptic realization, the CCS included one or more jets (intense current filaments) apparently meandering between counterrotating eddies.

We analyzed qualitatively an Advanced Very High-Resolution Radiometer infrared image (from the NOAA-7 satellite) of the SST field (1 August 1982) for an approximately 500-km square domain centered on the study area with only the predominant features schematized (Fig. 1). The general pattern is indicative of cool water upwelled at the coast in the summer season and of relatively warm water advected equatorward by the large-scale California Current. The band of cool water extending offshore from the coast and cutting through the CCS2 domain is a striking feature. This feature is also dominant in the SST map determined from the in situ XBT and CTD data; the SST map, in addition, indicates a sharp surface temperature front (2°C per 20 km; actually, 2°C per 5 km in continuous underway data) on the southern boundary of the cool feature. From the in situ data, the cool feature was about 30 m thick. Comparison of the dynamic topography and the SST maps confirms that the cool feature was coincident with the geostrophic jet, which had presumably advected the feature offshore from the coastal upwelling center off Point Arena. The cool feature entering the domain with the jet also appears in the infrared image. (There is apparently another cool feature in the image, cutting across the cyclonic eddy *C*. It may be a relic or may be controlled by some other mechanism. Alternatively, since there was a 3-day delay between the capture of the infrared image and the in situ sampling in that area of the domain, this cool feature may have been connected with the other one and, subsequent to the imaging, may have been displaced northwest with the cyclonic eddy.) Nearshore, near-surface drifters have documented (*6*) episodic offshore flowing jets in wind-driven coastal upwelling waters off Point Arena, consistent with the results described here.

In summary, a new conceptual picture of the CCS as a system of filamented jets meandering between synoptic-mesoscale cyclonic and anticyclonic eddies has emerged. The jet and eddy system can change substantially on a weekly time scale. The source of these eddies and their role in the local internal dynamics of the CCS (in either driving or damping the jets) have yet to be determined. This conceptual picture provides a mechanism (entrainment of cool water upwelled nearshore and subsequent offshore advection by jets and eddies) to explain the cool features commonly seen in satellite infrared imagery to extend far offshore from coastal upwelling centers. The advection of cool coastal waters to substantial distances offshore (100 km or more) has significance for the rapid (a few days) offshore transport of nutrients and biota associated with coastal upwelling and of pollutants discharged in the coastal ocean. The jets and eddies also advect warm offshore waters onshore to the coastal ocean. The implications of these results need to be incorporated in models of coastal ocean circulation, ecosystems dynamics, pollutant dispersal, fisheries, and climate.

CHRISTOPHER N. K. MOOERS
Department of Oceanography,
Naval Postgraduate School,
Monterey, California 93943

ALLAN R. ROBINSON
Center for Earth and Planetary
Physics, Harvard University,
Cambridge, Massachusetts 02138

References and Notes

1. W. S. Wooster and J. L. Reid, Jr., in *The Sea*, M. N. Hill, Ed. (Wiley, New York, 1963), vol. 2, p. 253; B. M. Hickey, *Prog. Oceanogr.* **8**, 191 (1979).
2. The California Cooperative Oceanic Fisheries Investigations Atlas Series.
3. J. L. Reid, Jr., and R. A. Schwartzlose, *J. Geophys. Res.* **67**, 2491 (1962); R. L. Bernstein, L. Breaker, R. Whritner, *Science* **195**, 353 (1977); H. P. Freitag and D. Halpern, *J. Geophys. Res.* **86**, 4248 (1981).
4. C. N. K. Mooers, S. A. Piascek, A. R. Robinson, *Ocean Prediction: The Scientific Basis and the Navy's Needs* (Proceedings of the Ocean Prediction Workshop, Monterey, Calif., May 1981).
5. R. D. Pillsbury, J. Bottero, R. E. Still, G. R. Heath, *Oreg. State Univ. Sch. Oceanogr. Rep. OSU-10* (1981); *Oreg. State Univ. Sch. Oceanogr. Rep. OSU-14* (1982).
6. R. E. Davis, "Current-following drifters in CODE" (Scripps Institution of Oceanography SIO Reference No. 83–4, La Jolla, Calif., April 1983).
7. M. M. Rienecker assisted in the data processing and in the critique of this report. The Office of Naval Research (Physical Oceanography Program) supported this research.

22 August 1983; accepted 21 September 1983

Structural and Bonding Changes in Cesium Iodide at High Pressures

Abstract. *Cesium iodide, a simple ionic salt at low pressures, undergoes a second-order transformation at 40 gigapascals (400 kilobars) from the cubic B2 (cesium chloride–type) structure to the body-centered tetragonal structure. Also, the energy gap between valence and conduction bands decreases from 6.4 electron volts at zero pressure to about 1.7 electron volts at 60 gigapascals, transforming cesium iodide from a highly ionic compound to a semiconductor. The structural transition increases the rate at which the band gap closes, and an extrapolation suggests that cesium iodide becomes metallic near (or somewhat above) 100 gigapascals. Similar changes in bonding character are likely to occur in other alkali halides at pressures above 100 gigapascals.*

Alkali halides are considered to be archetypal representatives of simple ionic bonding (*1*). Among these salts, CsI is of particular interest because its high compressibility allows the bonding forces to be probed over a substantial range of interatomic distances (*2*). The effect of pressure on ionic bonds should therefore be especially pronounced in this compound, and should not be obscured by crystal-structural transformations. This is because CsI at zero pressure is already in the high-pressure structure of the alkali halides: the B2 or CsCl-type structure (*3*). Indeed, on the basis of geometric packing, the B2 structure is thought to be the highest pressure phase accessible to the alkali halides (*3*). This is in accord with existing shock wave data that show no evidence for a first-order structural transition in CsI to a volume compression of 0.47 (*4, 5*).

Cesium iodide is isoelectronic with xenon, which has recently been the subject of considerable attention (*6*). The behavior of xenon and the other noble gases at high pressures is of theoretical interest because of the expectation that significant changes in bonding character occur under sufficient compression.